

CORSIKA Air Shower Simulations for the BLANCA Air Cherenkov Experiment

L. F. Fortson¹, J. W. Fowler¹, R. A. Ong¹, C. L. Pryke¹

¹*Departments of Physics and Astronomy, University of Chicago, Chicago, IL 60637, USA*

Abstract

Air shower simulations in support of the BLANCA air Cherenkov experiment using the CORSIKA code are described. Exploiting the thinning technique has allowed us to generate libraries of 10,000 showers with each combination of three primary types and four hadronic interaction models. It is demonstrated that a thinning level of 10^{-4} does not affect the parameters of interest. We have modified the CORSIKA code to include the atmospheric scattering of Cherenkov light by both the Rayleigh and Mie effects. The former effect dominates when considering the angle integrated lateral distribution.

1 Introduction

Observations of the lateral distribution of Cherenkov light produced by air showers can be used to study the composition of primary cosmic rays at energies around the knee ($\approx 10^{15.5}$ eV). The size of the electromagnetic cascade determines the total Cherenkov light intensity, while the depth of shower maximum controls the steepness of its lateral distribution. Heavier primaries shower higher in the atmosphere and produce flatter Cherenkov distributions. To draw quantitative conclusions from observed distributions it is necessary to model the air showers in detail. We have chosen the CORSIKA simulation code to interpret data from the CASA-BLANCA air Cherenkov experiment because it provides the most comprehensive choice of interaction models currently available.

BLANCA (Cassidy et al., 1997) consists of 144 angle-integrating Cherenkov detectors with a typical spacing of approximately 30 meters, located on the same site as the CASA surface array in Dugway, Utah (Borione et al., 1994). It is designed to study near vertical air showers, and each of its detectors views the sky only within 11° of the zenith. For each shower that triggers the scintillator array, BLANCA records the lateral distribution of Cherenkov light. It makes reliable measurements for primary energies as low as a few hundred TeV. These design parameters governed the zenith angle and energy range of the air shower libraries described here.

CORSIKA Version 5.61 (Heck et al., 1998), with the Cherenkov light option, produced the air shower simulations presented in this work. Four complete libraries of air showers were generated with each of the following high-energy hadronic interaction models: QGSJET, VENUS, SIBYLL, and HDPM. Each model was used with its corresponding set of cross sections. The libraries consist of 30,000 showers each, with equal numbers of proton, nitrogen, and iron primaries, and energies distributed uniformly in $\log E$ between 10^{14} and $10^{16.5}$ eV. The zenith angles are randomly chosen up to 12° from vertical with the appropriate distribution.

2 Thinning

A technique called thinning can be used to dramatically accelerate the simulation of air shower cascades. Below a threshold energy only a sub-set of the particles are tracked, with weightings to compensate for those discarded. The threshold is usually specified as a fraction of the primary energy, and referred to as the “thinning level.” Thinning reproduces the mean values of air shower observables but tends to increase their fluctuations. However, since intrinsic fluctuations are large, it is possible to run the simulations with very severe thinning and still obtain adequate results. This means that many showers can be generated over a multidimensional grid of primary parameters and shower models within an acceptable computing time. An optional thinning algorithm has been included in the CORSIKA code since version 5.2, and we use it in this work.

CASA-MIA measures electron and muon shower size at ground level (N_e and N_μ). BLANCA measures the Cherenkov lateral distribution which we parameterize by the light intensity at 120 m (C_{120}), and the exponential slope (s) in the range $30 < r < 120$ m. In addition, we are interested in the depth of shower maximum

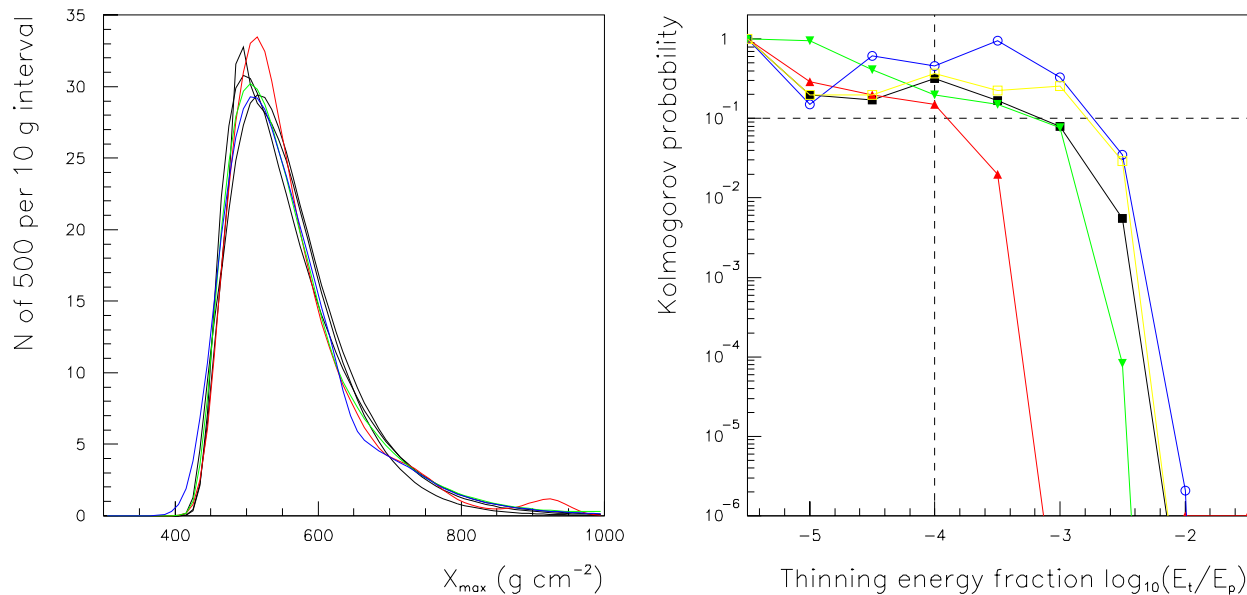


Figure 1: *Left*: 500 shower distributions of X_{max} for thinning levels from $10^{-5.5}$ to $10^{-3.0}$. *Right*: Probability of compatibility between distributions of X_{max} , N_e , N_μ , C_{120} and s versus thinning level comparing to the $10^{-5.5}$ set.

(X_{max}), as this parameter is widely calculated and discussed in the context of air shower composition experiments.

To determine the maximum acceptable thinning which still produces showers of adequate quality for our purposes, sets of 500 events each were generated at thinning levels of $10^{-1.5}$ to $10^{-5.5}$ in half decade steps. The primaries were 10^{15} eV protons, and the QGSJET model was used. The resulting parameter distributions appear to be very similar — see the left panel of Figure 1. To make a quantitative test, the Kolmogorov probability was computed in each case comparing against the $10^{-5.5}$ thinned set. The results are shown in the right part of the figure; for thinning levels below $10^{-4.0}$, and 500 event sets, the distributions are statistically indistinguishable. The parameter which shows considerably more sensitivity to thinning than the rest is N_e . In the light of this study a thinning level of $10^{-4.0}$ was selected for shower library generation.

3 Models of Atmospheric Scattering

A single angle-integrating Cherenkov detector, such as a BLANCA unit, detects light emitted at a range of altitudes. To account properly for the transmission of Cherenkov light through the atmosphere, the air shower simulation must model atmospheric scattering. We have added the effects of both molecular and aerosol scattering of Cherenkov photons to CORSIKA in order to produce the most realistic Cherenkov lateral distributions possible.

Rayleigh scattering refers to the elastic scattering of light by neutral gas molecules in the atmosphere. The cross section for this process is proportional to the gas density, so it depends on the same density profile that governs the air shower development. Light with a wavelength of 400 nm has a mean path length for Rayleigh scattering of 2970 g cm^{-2} . This is small compared with the observation depth at Dugway (870 g cm^{-2}), but even so, some photons will scatter. The path length increases as $X_R \propto \lambda^4$, so Rayleigh scattering is much more important for the shorter blue and UV wavelengths. The angular distribution of scattered light is symmetric forwards and backwards, with $\frac{d\Omega}{d\theta} \propto (1 + \cos^2 \theta)$. Light generally scatters through large angles, and is equally likely to emerge from an encounter heading upwards or downwards. Since photons are unlikely to re-scatter, a scattered photon usually does not reach the detector array.

We also model the Mie scattering process, caused by aerosol particles suspended in the atmosphere.

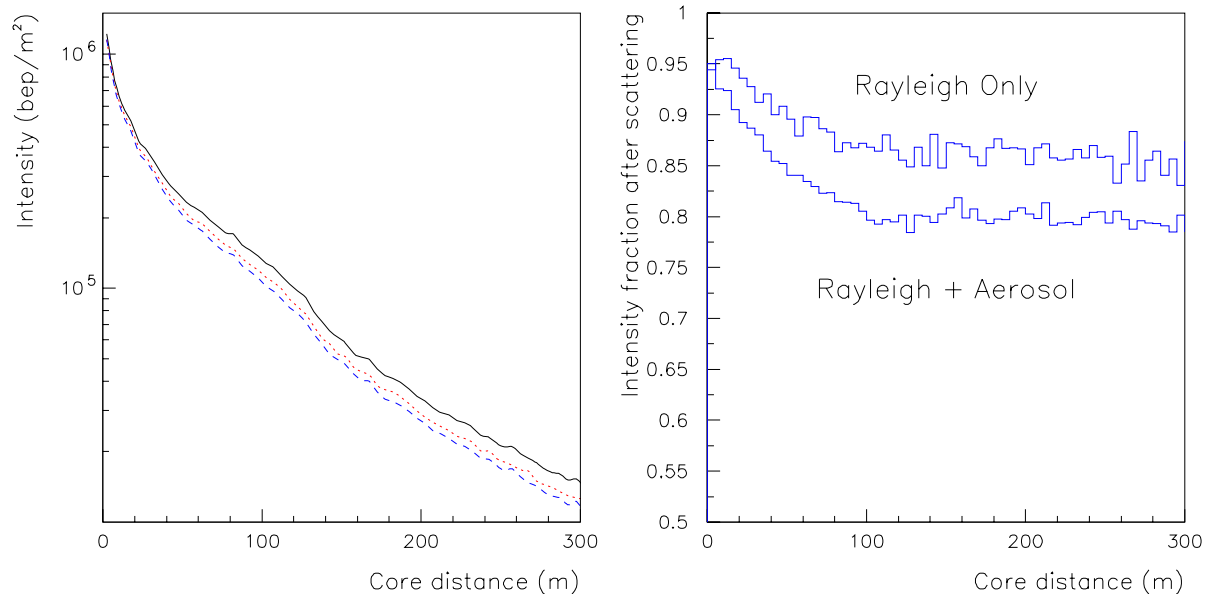


Figure 2: *Left*: Cherenkov lateral distribution of an example shower; no scattering, Rayleigh scattering only, and Rayleigh plus Mie scattering. *Right*: fractional loss due to scattering increases with core distance.

Aerosol concentration varies substantially at different locations and times; so can the distribution of particle sizes. For the sake of simplicity, we use an empirical model for Mie scattering that represents typical conditions at BLANCA’s desert site (Sokolosky, 1989). Since we find that the Rayleigh process actually dominates the scattering of Cherenkov light, this simple aerosol model suffices. The scale height of aerosol particles (1.2 km) is much shorter than that of the atmosphere (typically 8 km), so Mie scattering tends to occur much closer to the ground than Rayleigh scattering does. The model assumes that the scattering path length at the ground is 14 km for light with a 400 nm wavelength but depends only weakly on wavelength. Thus, we adopt a path length that increases as $\ell \propto \lambda^{1.3}$. Also, Mie scattering is peaked in the forward direction, unlike molecular scattering, and we assume an angular distribution of the form $\frac{d\Omega}{d\theta} \propto e^{-\theta/27^\circ}$.

Our algorithm tracks photons even after they scatter, using the angular distributions given above. Molecular scattering, which tends to happen high in the atmosphere and is almost isotropic, generally redirects photons out of the detector area entirely. However, due to the relatively low altitude of the dust layer, Mie scattering occurs near the observation level. Low-altitude scattering, and the forward-peaked angular distribution, mean that particles scattered by aerosols can still land in the main pool of Cherenkov light. For a detector array with large angular acceptance, these scattered photons could distort the Cherenkov lateral distribution. However, BLANCA’s narrow field of view ($\approx 11^\circ$) makes it less sensitive to scattered light.

4 Effects of Atmospheric Scattering on Cherenkov Distributions

The effect of atmospheric scattering on Cherenkov measurements is small in the showers that BLANCA observes. Only 20% of the photons scatter in an average vertical 1 PeV air shower. Scattering would be a more important effect for cosmic rays of lower energy or at larger zenith angles, because such showers develop further from the observation site, and hence the Cherenkov light passes through more intervening atmosphere. Among the photons reaching the ground from a 1 PeV shower, there are an average of 0.24 scatters per photon. Two-thirds of these scattering events are due to the Rayleigh process.

By reducing the number of Cherenkov photons reaching the detectors, atmospheric scattering alters the

absolute energy calibration. Figure 2 shows that, except near the shower core, the two scattering processes combined reduce the Cherenkov intensity uniformly by 20%. If scattering were ignored BLANCA would systematically underestimate primary energies by about that amount. The light lost due to scattering changes very slowly with shower energy. More energetic primaries produce showers that penetrate deeper into the atmosphere, so slightly less of their Cherenkov light is lost because of scattering.

In addition to reducing the total amount of light, atmospheric scattering also changes the shape of the observed Cherenkov lateral distribution. This happens because light at different core distances has traversed different amounts of atmosphere. Most light arriving more than 100 meters from the shower core is emitted between 2 and 6 km above the surface, *i.e.* near shower maximum. However, Cherenkov light observed exactly at the shower core is emitted much nearer to the observation level, most of it less than 2 km above the ground. Therefore, scattering loss is less severe near the core, steepening the observed slope in the Cherenkov lateral distribution (Figure 2).

The Cherenkov lateral distribution shape is used to infer the primary mass. In particular, the exponential slope of the distribution within 120 meters of the core (the “inner slope”) is an almost linear indicator of the depth of shower maximum. The combined effects of both types of atmospheric scattering increase the inner slope by about 0.8 km^{-1} , making all showers appear to have deeper X_{max} and seem more proton-like. However, at any given energy the slope change due to scattering is much smaller than the average difference between protons and iron, which is typically 5 km^{-1} (Figure 3). Including the effects of scattering will therefore increase the inferred primary mass, but only slightly.

5 Conclusions

The interpretation of air shower data relies heavily on simulations. We have shown that the thinning level used in the production of our event libraries does not alter the results and allows us to achieve high statistics. We have improved the accuracy of the CORSIKA code by including the Raleigh and Mie scattering of Cherenkov photons. The Raleigh process dominates in our circumstances, which is fortunate because it can be modelled more accurately than the variable aerosol effect. The combined scattering processes lead to a systematic increase of around 20% in inferred primary energy, but have smaller effects on mass.

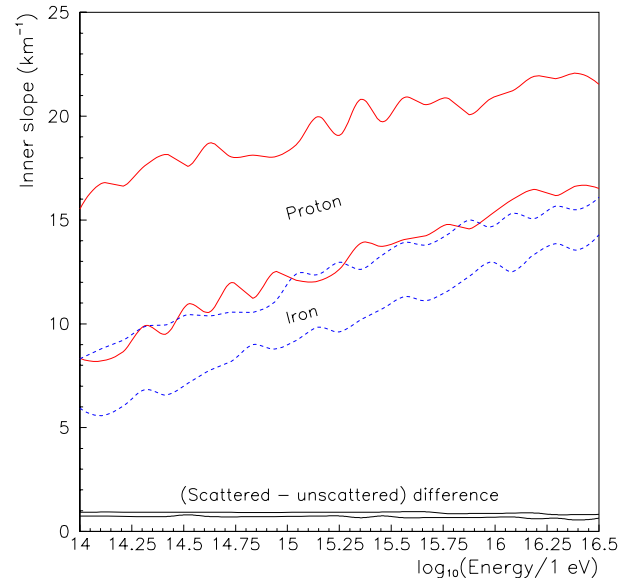


Figure 3: The range of Cherenkov inner slope values for proton and iron primaries, as well as the slope increase due to Rayleigh and aerosol scattering.

References

- Borione, A. et al., 1994, Nucl. Instr. Meth. A 346, 329
- Cassidy, M. et al., Proc. 25th ICRC (Durban, 1997) OG 10.3.32
- Heck, D. et al., 1998, Report FZKA 6019 Forschungszentrum Karlsruhe
- Sokolsky, P. 1989, Introduction to Ultrahigh Energy Cosmic Ray Physics (Addison-Wesley)